Design of Human Knee Smart Prosthesis with Active Torque Control

Oscar Arteaga, Héctor C. Terán, Hernán Morales V., Edison Argüello M., María I. Erazo, Marcelo Ortiz and Jonathan J. Morales
Universidad de las Fuerzas Armadas ESPE, Sangolquí, Ecuador
Email: obarteaga@espe.edu.ec, {hcteran, hvmorales, eoarguello, mierazo, amortiz8, jjmorales7}@espe.edu.ec

***Abstract*— This study presents the results of an investigation of Magnetorheological fluids used in the implementation of a knee prosthesis prototype with active movement control and stability in posture, when replacing lost muscle function for people with transfemoral amputations. A magnetorheological torque limiter was used to implement a prosthetic knee device with adjustable torque applied to the join. This was achieved by using a magnetorheological fluid (MRF) brake lord MRF – 140 CG as actuator. This prosthesis includes rotation lock, an impact attenuator to simulate the natural action of normal knee flexion, and torque regulation to provide maximum safety and a normal walking movement. The prototype has a control for the adjustment of the magnetic field applied to the MRF, thus successfully emulating human march of the prosthesis in different positions.**

***Index Terms*—magnetorheological fluids, smart materials, torque limiter, knee prosthesis.**

I. Introduction

Currently the number of people who have undergone an amputation procedure in lower extremities has grown in the last decade [1]. The high incidence produces a growing demand for devices such as prostheses for sectors of the population with disabilities in the lower extremities. [2]. In Ecuador, from 2007 to 2013, approximately 875 cases of traumatic lower extremity amputations were performed, and this number is expected to increase [3]. According to data from INEC in 2011, diabetes mellitus was the main reason for death in Ecuador and subsequent amputations in lower limbs [4].

Similarly, this is the main motivation for companies and institutes to work on the development of functional prototypes [3]. Areas, such as robotics, that encompass different disciplines in the design of multidisciplinary systems [5] help to develop prosthesis with better technology than in past years.

The amputated limb function can be restored through a robotic prosthesis by adjusting impedance parameters in different stages of walking, as well as regulating the dynamic parameters according to the environment where the patient is using the prosthesis [6]. The robotic prosthesis and exoskeleton will provide natural mobility, dexterity and sense of touch to the paralyzed or missing limbs [7, 8, and 9].

Manuscript received July 28, 2018; revised October 11, 2019.

Many devices that use magnetorheological fluids (MRF), such as brakes and clutches, have been developed for both industrial applications and biodevices [10, 11, 12], providing active control of movement and attenuation of impacts [13]. However, these require improvements regarding thermal conductivity and this is achieved by a more efficient thermos-magnetic convection [14]. Also, in recent years, the development of lower extremity prosthesis has had a growth, including knee prosthesis [15, 16, 17], which through MRF studies [14, 18], are proposed as functional prototypes that can adapt themselves in real time to the human march cycle.

II. Kinematics of the Human Knee

The femorotibial joint presents a movement with six degrees of freedom [19], the range of motion in the sagittal plane is greater than in the rest of the planes. For this reason, the movement study was done in a simplified manner on the mentioned plane, the location of the marker and the angles of the limbs and joints are made by means of an established convention.

The angles of the extremities in the spatial reference system are determined counterclockwise from the horizontal as positive which can be described the angle of knee as a combination of two angles where θ_1 corresponds to thigh angle and θ_2 to the shank angle as seen in Fig, 1.

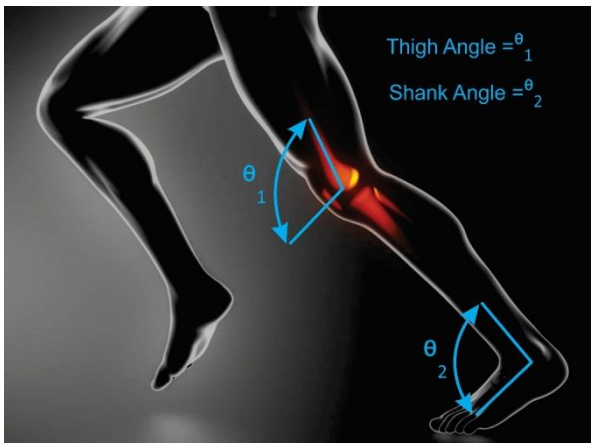

Figure 1. Angles of the limbs

To obtain the value of the angle of the knee, equation 1 was used.

$$\theta_{knee} = \theta_1 - \theta_2 \quad (1)$$

doi: 10.18178/ijmerr.9.3.347-352

When the θ_{knee} values are positive, they correspond to the flexion state and when the values are negative, they show a state of extension in the knee.

III. MRF Fluid

MRFs are a type of intelligent material whose characteristics change rapidly and can be easily controlled by the application of an external magnetic field. The change is proportional to the intensity of the applied magnetic field, as it is shown in Fig. 2.

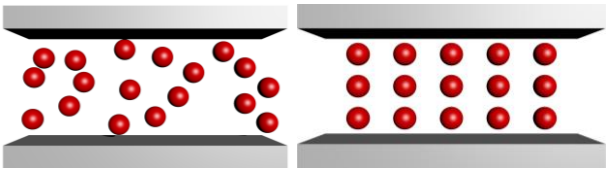

Figure 2. Behavior of a MRF: a) In the absence of a magnetic field; b) In the presence of a magnetic field

The MRF used in this study case was the LORD MRF - 140CG, it presents characteristics that are suitable for flow limit control to the cut and viscosity, properties which are important to consider in this type of applications [20].

IV. Analysis of MRF Mechanical Properties

To determinate the mechanical and rheological properties of the MRF – 140 CG, tests were carried out using a rotational rheometer MRC-501, equipped with a magnetorheological cell MRD -70/1T coupled for the application of the variable magnetic field. Temperature control was done through a Julabo F-25 thermostatic bath. In the tests carried out with shear velocities of up to 350 s-1, a pseudoplastic behavior of the MRF was observed as the temperature and viscosity values also increased.

Data from the shear stress tests were taken at 20 ℃, obtaining the curve shown in Fig. 3, whose slope represents the magnetorheological fluid MRF – 140 CG viscosity.

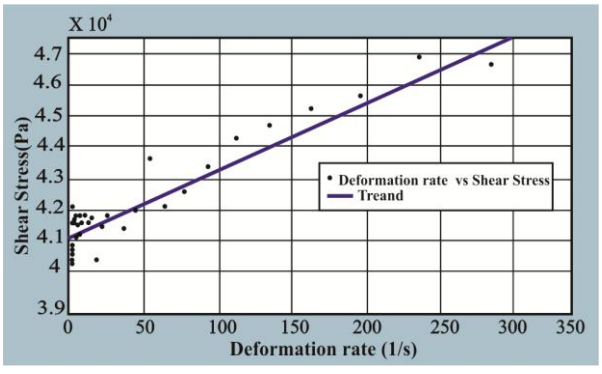

Figure 3. Approach curve Shear strength vs Deformation Rate

The trend equation is obtained by linear regression techniques, and is given in (2):

$$y = 21.51x + 4.107.10^4 \quad (2)$$

From where viscosity of the MRF is 21.51 (Pa.s) was determined.

In addition, from the test performed, there is considerable variation in the magnetic field, the value in the MRF shear stress increases as shown in Figure 4, and presents a shear behavior in different magnetic field values

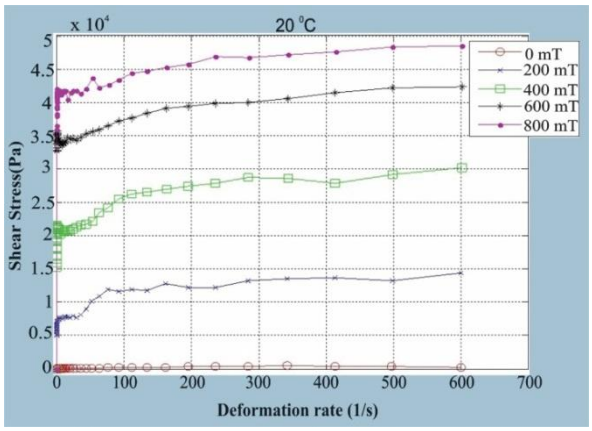

Figure 4. Shear stress depending on the magnetic field

A similar behavior is observed in Fig 5, in which there is an increase in the shear threshold which increases in the presence of a magnetic field and with an increase in temperature. Fig. 5 shows the variation of shear stress obtained at different temperature ranges with magnetic fields fluctuating from 0 T to 0.8 T. There are few differences in MRF behavior at different temperatures.

The results obtained show the increase of the shear threshold according to the intensity of the magnetic field for the four temperatures analyzed. In addition, there are few differences between the different temperatures.

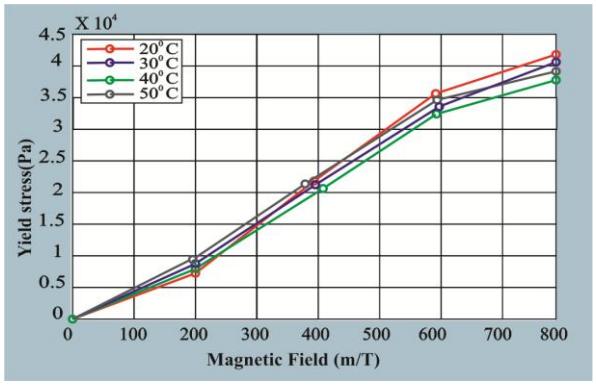

Figure 5. Shear threshold in function of the magnetic field and temperature

V. Mechanical Design

According to a comparative statistical study of anthropometric measurements among whites, mestizos, indigenous people in the world [21], the average height for men is between (1.67 a 1.70) m. Men mass varies between the values of (65 a 70) kg approximately, being this the load that the structure of the prosthesis must support along with its components.

In this section a torque limiter, a transmission system, the support of the limiter, and the prosthesis structure are designed under the principles of theoretical and computational mechanics, where each of the

considerations is detailed in the static and dynamic analysis of each element.

The torque transmission of the limiter is quite dependent on the shear limit and the viscosity of the fluid. The Bingham plastic model is used to predict the behavior of MRF in the actuator used in direct cut mode, and is given in (3):

$$\tau(r,\omega,H) = \tau_y(H) + \eta\frac{\omega r}{h} \quad (3)$$

where τ (r, ω, H) is the cutting force, which depends on the radius r, the angular velocity ω and the magnetic field strength H. τ_y (H) is the dynamic performance limit that depends on magnetic flux density, viscosity of the fluid η, angular velocity of the rotating disc ω, thickness of the fluid passage channel (gap) h, and radius of the outer surface of the disc r, represented in Fig. 7 by R_2. The resistive torque can be found by differentiating the shearing force along the dish surface see in (4) [22].

$$T = 2\int_{R_i}^{R_0}(\tau_y(H)2\pi r)rdr \quad (4)$$

T is the resistance pair, R_i y R_0 are internal and external radius respectively. Substituting the (4) in (3) the following equation is obtained (5):

$$T = \frac{4\pi}{3}\tau_y(H)\left({R_0}^3 - {R_i}^3\right) + \frac{\eta\omega\pi}{h}\left({R_0}^4 - {R_i}^4\right) \quad (5)$$

As you can see in (4), the torque consists of two terms: one includes MRF and the other is related to viscous flow. The MRF torque limiter is designed to work at very small rotation speeds, so the contribution of viscosity is very small and can be discarded compared to the effects of fluid, thus considering only the first term for the design. The maximum yield strength in the linear work area is *E* = 42 kPa and the magnetic field is H = 100 kA/m. The diameter selected for the shaft is 12.7 mm, Ri = 6.35 mm. Through the calculations, it was determined that the maximum torque that the torque limiter can resist is 4.7 Nm.

The torque required during the march of the person must be minimum of 25Nm [6] while the maximum torque delivered by the servo motor is 4 Nm. It is necessary to multiply this value by a transmission ratio of 6.25:1. The transmission of power and torque will be done by means of straight gears as shown in Fig. 6, therefore it is required to design a transmission system that allows to multiply the torque provided by the servomotor.

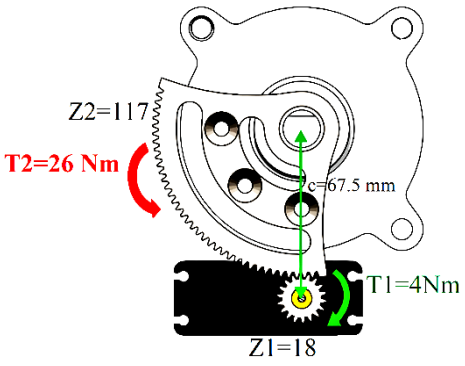

Figure 6. Transmission Ratio

With this transmission ratio, is obtained an output torque on the axis of rotation of: 4 [Nm] x6.5 = 26 [Nm], which satisfies the 25 [Nm] required during human walking; also if we consider that the torque limiter gives us a torque of 5 [Nm] and due to the two devices (servo and limiter) we work together during the whole cycle, it can be said that it can obtain a maximum braking torque in the joint de 31Nm by the equation (6).

$$T_{max}joint = T_1 + T_{limiter} = 31Nm \quad (6)$$

A. Shear Stress Limiter

The actuator operates in direct switch mode by cutting the MRF that is in the gap. As the viscosity of the MRF changes in the presence of an excited magnetic field around the coil, the torque will change.

R_i represents the torque limiter shaft radius, R_2 is the disc radius, R_3 is the distance from the shaft to the end of the coils, R_0 represents the torque limiter outer radius while *a* represents its width, as shown in the Fig. 7.

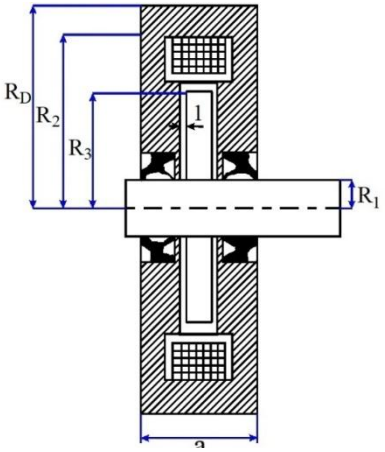

Figure 7. Dimensional parameters of the torque limiter

B. Magnetic Circuits with MRF

The magnetomotive force NI is obtained from the Ampere law, NI = ∮Hdl, where the magnetic constant of iron is much higher (1000 times) than the MRF (μ_{Fe} >> μ_{MR}). The integral is dominated by the contribution of the gap. [24]

Considering a cast iron core that has a constant cross section (A_{Fe}) with a coil rolled in a small portion of it, it represents a circuit that is equivalent to Kirchoff's voltage law as shown in Fig. 8.

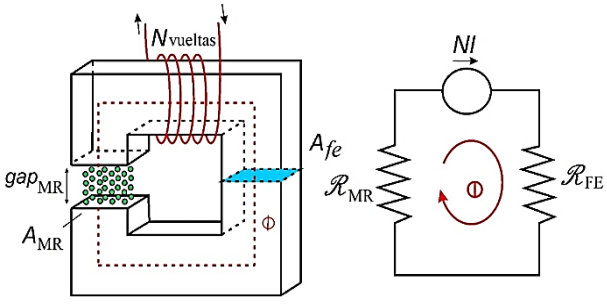

Figure. 8. Magnetic core with gap of MRF: a) magnetic circuit – b) equivalent electrical circuit

Kirchhoff's equivalent voltage law shows (7):

Where: $$NI = (R_{MR} + R_{Fe})\Phi \quad (7)$$

The iron material is replaced by the steel material because the torque limiter is manufactured in steel, obtaining (8):

$$H_{MR} = \frac{\Phi}{\mu_{MR} A_{MR}} = \frac{NI}{g_{MR} + l_{acero}(\frac{\mu_{MR}}{\mu_{Fe}})(\frac{A_{MR}}{A_{Fe}})} \quad (8)$$

VI. Electronic Design

To perform control of the knee prosthesis, the human walking cycle model is considered in the study of anthropometry conducted in the investigation of the knee prosthesis control system model for a walking cycle [23]. The behavior of the knee was simulated by means of an algebraic regression under the parameters described in Fig. 9.

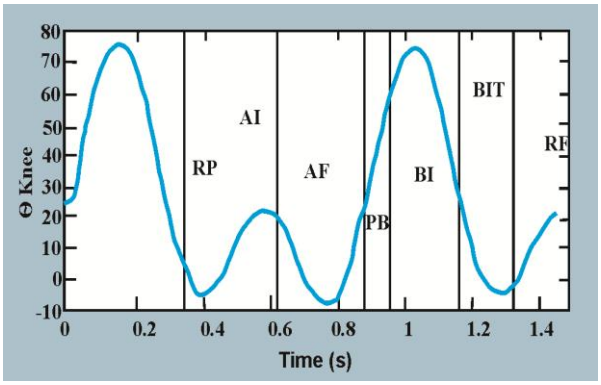

Figure 9. Graph of the angular variation in degrees of the joint of the knee prosthesis. RP- response to weight, AY- intermediate support, AF- final support, PB- pre swinging, BI- initial swinging, BIT- intermediate swinging, BF- final swinging.

Fourier's equation is used to predict the knee kinematic behavior according to the angles. A margin of error less than 2% was obtained by (9).

$$\theta(t) = 23{,}06 - 18{,}24cos(3{,}06t) + 13{,}2sen(3.06) + 3.94cos(6.11t) - 21.35sen(6.11t) \quad (9)$$

A. Accelerometer ADXL335

This device interprets the angle at which the knee is located during the entire walk cycle and generates an analogue signal that provides information regarding prosthesis Where I current = 0.8 A, g_{MR} (gap) where the fluid is = 1mm, l_{steel} magnetic length of the steel = 0.213 m, μ_{MR} coefficient of magnetic permeability of the fluid MR= 5.26, μ_{steel} magnetic permeability coefficient of steel = 100 (Olmo, 2012), A_{MR} Fluid area = 0.131 m^2, A_{steel} Steel area = 0.444 m^2, H_{MR} Magnetic field strength of the fluid = 121000 A/m. Resulting n 216 turns of wire 24 AWG.

The magnetic design involves both the mechanical and electronic stages, each consisting of components have a direct or indirect relationship between them according to their nature and function, shown in Fig. 10.

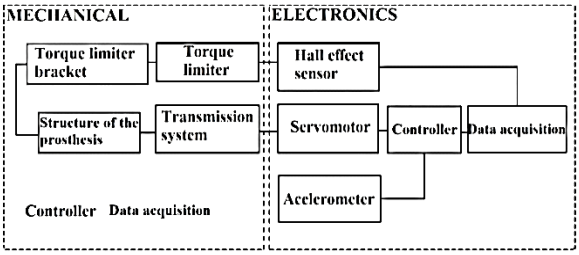

Figure 10. Electronic and mechanical scheme of the prosthesis.

B. Arduino ONE R3

Performs analogue input reading and processing according to the established algorithm set to activate PWM outputs that are sent to the actuators

C. Sabertooth 2x5

DC Motor Controller board capable of establishing RS232 serial communication point to point with the control board, allowing greater communication speed and better control of the outputs to the actuator and to the torque limiter. Provides up to 5A per output and withstand peaks up to 10A.

D. Hall Effect sensor

Used to determine the position or speed of devices. Two sensors of this type were integrated, which are used to carry out the feedback to the control algorithm PI on the controller board. Each sensor is at 90 °of the other.

E. Li-Po Battery

This type of battery is used to provide the necessary current to power devices, such as the torque limiter that requires a high current. Its operating voltage is provided by 3 cells with 2200mAh capacity.

F. Controller Design

Once the signals provided by the electronic components were determined through a closed-loop proportional-integral (PI) controller scheme, the numerical value of the accelerometer is taken as the set point and input to the system. Actuators (actuators and limiters) of torque) enter act according to the value provided by the PI controller. Figure 11 shows the control diagram of the system.

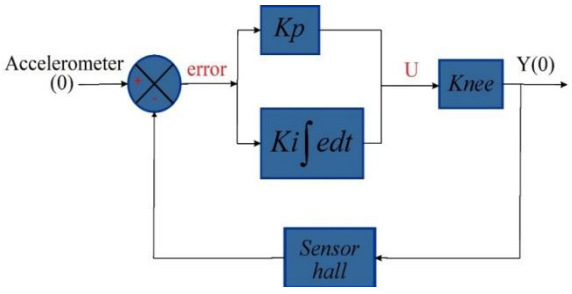

Figure 11. System control diagram

The PI controller relates the angle provided by the accelerometer in a n instant of time during the cycle of the walk with the actuator movement. The controller then performs a comparison between the positions of the torque limiter axis with the help of the Hall Effect sensors,

obtaining the error entering the controller in order to send a new output to the actuators.

The proportional part of the controller acts by rapidly sending the actuator to the desired position, while the integral part of the controller is in charge of stabilizing the error in stable state. That is, the closer the system gets to the desired angle value, the smaller the control signal becomes, trying to always stabilize the system at the desired value.

According to all subsequent analyses and calculations, it has been ensured that each element that makes up the prototype knee prosthesis meets the design requirements, so that the final design has remained as shown in Fig. 12, with all its mechanical and electronic components.

Figure 12. Knee prosthesis prototype

VII. Tests and Results

One of the important points in the prosthesis is the torque limiter, so it was essential to determine the real torque that it can support because the mathematical models data provided by the manufacturer has an unknown efficiency. For this, an arm of 15 cm with a negligible weight and certified weights of both 0.5 kg and 2 kg were used to determine rotation angles as well as torques obtained during motion tests.

Once subjected to the limiter, the arm and mass of 0.5 kg were placed, which required a current of 0,2 A to move de load. This generated a torque of 0.86 Nm.

In Fig. 13 the real behavior of the torque limiter is compared with the data proposed by the manufacturer, this was obtained by varying the mass and the current. In the ideal a proportional increase of the torque with the current from 0.4 [A] to 0.8 [A] is observed, which differs from the real one carried out in the laboratory, which shows an exponential relation between the torque and the current.

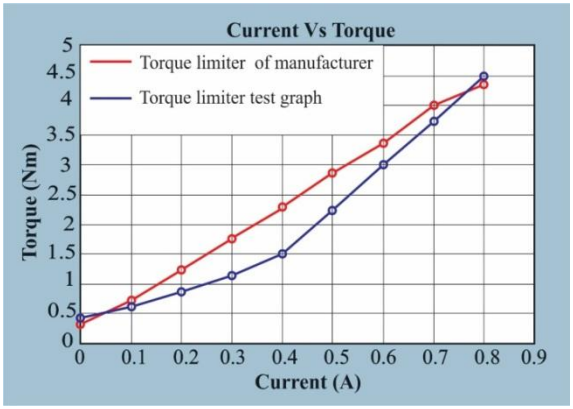

Figure 13. Current Vs Torque

A. Response of the Prosthesis during Operation

To carry out the human gait analysis, the data were taken using the MATLAB and Arduino software. When comparing the referential graph of the human gait in Fig.14 (blue) and the data obtained in the tests shown in Fig.14 (red), it is observed that the behavior of the prosthesis is similar. In Fig. 13, the actual behavior of the torque limiter is compared with the data proposed by the manufacturer, this was obtained by varying the mass and current. In the ideal it is observed a proportional increase of the torque with the current of 0.4 [A] to 0.8 [A], which differs from the real realized in the laboratory, which shows an exponential relation between the torque and the current. A small delay due to data transmission must also be taken into account, however, it does not significantly affect the response of the system.

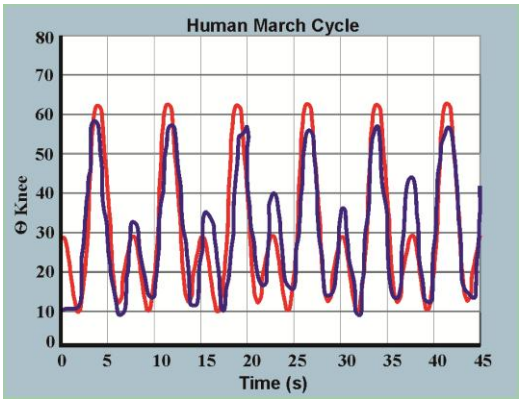

Figure 14. Human march obtained, functional prosthesis, vs function of human referential march

VIII. Conclusions

With the help of rheological analysis it can be determined that apparent viscosity of the MRF-140 CG fluid is directly influenced by the applied magnetic field showing a value of 21.6 Pa.s, in addition to a shear of 41.7 kPa with an active magnetic field of 0.8 T.

Rotation speed of the knee in the prosthesis is affected by the speed of the actuator and by the high torque required during a normal walk. However, as this is a prototype, its performance successfully complies with the reference graph of human walk.

For a correct design of the torque limiter it is necessary to consider three important parameters, such as the number of turns of the internal coil, the magnetic saturation limit and the cavity where the fluid is stored (gap), since the variation of any of these parameters directly influence the experimental theoretical torque that the device will have.

The torque limiter of MRF used to generate the initial torque on the walk, presents at initial torque when the input current is 0 A, that is, in the off state it has an initial viscosity and when it encounters a maximum magnetic field of 100 kA, it has a torque of 4.7 Nm.

Because magnetorheological devices require a magnetic field for their control, they are controlled electronically, so that it is possible to use algorithms with feedback improving their functionality and their response speed.

CONFLICT OF INTEREST

The authors declare no conflict of interest.

AUTHOR CONTRIBUTIONS

Oscar Arteaga conducted the research; Héctor C. Terán built the prototype; Edison Arguello M. realized the cinematic and CAE analysis of the prosthesis; Hernán Morales V. wrote the mechanical content the paper; María I. Erazo wrote electronic content the paper; Marcelo Ortiz carried out the execution of function tests and Jonathan J. Morales analyzed the data obtained from the tests carried out on the prototype. All authors had approved the final version.

REFERENCES

[1] D. A. José, Design of a leg prosthesis for transtibial amputees, (2015).
[2] M. Ulises Rafael, Design and construction of a modular orthopedic prosthesis for transtibial amputee, (2006).
[3] G. Andrés, C. Luis, Design and construction of lower limb prostheses monitored from a personal computer, (2015).
[4] U. Héctor, Z. Edgar, Design, construction and implementation of mechanical ankle prostheses with three degrees of freedom, (2016).
[5] C. Fragassa., L. Berardi, G. Balsamini, Magnetorheological fluid devices: an advanced solution for active control. Faculty of Mechanical Engineering, (2016).
[6] J. García, C. Rodríguez, Design of a transtibial cushioned prosthesis. México DF. México: Instituto Politécnico Nacional, (2012).
[7] M. Gonzales, & et. al, Lower extremity amputation and disability. Prosthesis and Rehabilitation. Barcelona: Masson, (2005).
[8] V. Ragusilaa, M. R. Emami. "Mechatronics by analogy and application to legged locomotion," *Mechatronics, Inform. Process*, 2016, pp. 1–19.
[9] M. R. Tucker, J. Olivier, A. Pagel, H. Bleuler, M. Bouri, O. Lambercy, José del R Millán, R. Riener, H. Vallery, R. Gassert, "Control strategies for active lower extremity prosthetics and orthotics: a review," *Journal of NeuroEngineering and Rehabilitation*, 12, 2015.
[10] G. Fei, Yan-Nan L, Wei-Hsn L, Optimal design of magnetorheological damper used in Smart prosthetic knees, (2017).
[11] H. Zhan, C. Liao, W. Chen, S. Huang, A magnetic design method of MR fluid dampers an FEM analysis on magnetic saturation, (2006).
[12] J. Kwon, P. Eric, Evaluation of magnetorheological fluid augmented fabric as a fragment barrier material, (2012).
[13] G. Dirk, S. Markus, M. Jurgen, Magnetic fluid control for viscous los reduction of high-speed MRF brakes and clutches with well-defined fail-safe behavior, (2013).
[14] M. S. A. Rahim, I. Ismail, Review of magnetorheological fluids and nanofluids thermal behavior, 2015.
[15] X. Lei, W. Dai-Hua, F. Qiang, Y. Gang, H. Lei-Zi, A novel four-bar linkage prosthetic knee based on magnetorheological effect: principle, structure, simulation and control, 2016.
[16] J. Chen, W. Liao, Design, testing and control of a magnetorheological actuator for assistive knee braces, 2010.
[17] F. Qiang, W. Dai-Hua, X. Lei, Y. Gang, A magnetorheological damper-based prosthetic knee (MRPK) and sliding mode tracking control method for an MRPK-based lower limb prosthesis, 2017.
[18] G. Chaoyang, G. Xinglong, X. Shouhu, Y. Qifan, R. Xiaohui, Squeezq behavior of magnetorheological fluids under constant volumen and uniform magnetic field, 2013.
[19] S. Cervero, J. Honrado, G. Monzó, S. Rodriguez, Biomechanics of the knee, Pathology of the locomotor system, 2005.
[20] Daniela R, Ladislau V, Yield stress and Flow behavior of concentrated ferrofluid-based magnetorheological fluids: the influence of composition, (2014).
[21] Au, Samuel K., Weber J., Herr H., "Powered ankle--foot prosthesis improves walking metabolic economy," *IEEE Transactions on Robotic*s, 25, 2009, pp. 51-66.
[22] Martinez-Villalpando, Ernesto C., Mooney L., Elliott G., Herr H. Antagonistic active knee prosthesis. A metabolic cost of walking comparison with a variable-damping prosthetic knee. In Engineering in Medicine and Biology Society. 2011, pp. 8519-8522.
[23] H. M., L., G., S., C., G., & C., K. Reliable Plate-Plate MRF Magneto-Rheometry Based on Validated Radial Magnetic Flux Density Profile Simulations. Rheo, (2008).
[24] R. J. Farris, H. A. Quintero, S. A. Murray, K.. H. Ha., C. Hartigan, M. Goldfarb, "A preliminary assessment of legged mobility provided by a lower limb exoskeleton for persons with paraplegia," *IEEE Transactions on neural systems and rehabilitation engineering*, vol. 22, 2014, pp. 482-490.